Imperfections in Focal Conic Domains: the Role of Dislocations

Maurice Kleman, Claire Meyer, Yuriy A. Nastyshyn

Imperfections in Focal Conic Domains: the Role of Dislocations

Journal:	*Philosophical Magazine & Philosophical Magazine Letters*
Manuscript ID:	TPHM-06-Feb-0033.R1
Journal Selection:	Philosophical Magazine
Date Submitted by the Author:	20-Mar-2006
Complete List of Authors:	Kleman, Maurice; Université Pierre-et-Marie-Curie, IMPMC Meyer, Claire; Université de Picardie Jules Verne, Laboratoire de Physique de la Matière Condensée Nastyshyn, Yuriy; Institute of Physical Optics
Keywords:	disclinations, dislocations, liquid crystals, phase transitions
Keywords (user supplied):	focal conic domain, kink

Imperfections in Focal Conic Domains: the Role of Dislocations

M. Kleman[1], C. Meyer[2], and Yu. A. Nastishin[1,3]

[1]Institut de Minéralogie et de Physique des Milieux Condensés (UMR CNRS 7590),
Université Pierre-et-Marie-Curie, Campus Boucicaut,
140 rue de Lourmel, 75015 Paris, France

[2]Laboratoire de Physique de la Matière Condensée, Université de Picardie,
33 rue Saint-Leu, 80039 Amiens, France

[3]Institute of Physical Optics, 23 vul. Dragomanova, Lviv 79005, Ukraine

ABSTRACT.

It is usual to think of Focal Conic Domains (FCD) as perfect geometric constructions in which the layers are folded into Dupin cyclides about an ellipse and a hyperbola that are conjugate. This ideal picture is often far from reality. We have investigated in detail the FCDs in several materials that have a transition from a smectic A (SmA) to a nematic phase (N). The ellipse and the hyperbola are seldom perfect, and the FCD textures also suffer large transformations (in shape or/and in nature) when approaching the transition to the nematic phase, or appear imperfect on cooling from the nematic phase. We interpret these imperfections as due to the interaction of FCDs with dislocations. We analyse theoretically the general principles subtending the interaction mechanisms between FCDs and finite Burgers vector dislocations, namely the formation of *kinks* on disclinations, to which dislocations are attached, and we present models relating to some experimental results. Whereas the principles of the interactions are very general, their realizations can differ widely in function of the boundary conditions.

PACS numbers: 61.30Jf, 61.72Lk

I. INTRODUCTION

The discussion that follows, about the behavior of defects in the SmA (smectic A) phase is inspired by a few experimental polarized light microscopy observations reported in [1] and summarized below. These observations have since been developed [2]. They relate to a domain of temperature that extends approximately $1°C$ below the SmA $\rightarrow$ N phase transition, some of the most relevant experiments having been done with an accuracy of ±1mK. The very near vicinity of the transition, where phenomena usually qualified of transitional do happen, could not be investigated, and then has not been. It appears, in the domain we have searched, that the focal conic domains suffer considerable visible modifications, with remarkable imperfections in shape. It is the nature of these imperfections that we wish to describe in the present article.

The defects and textures of the SmA and N phases are reasonably well understood at mesoscopic and macroscopic scales, at least for their static physical and topological properties. Contrariwise, the role played by the smectic defects at the phase transition has been little investigated. It is precisely in this region that the FCDs (focal conic domains), the only defects that are fully observable in light microscopy, show these large modifications that, we shall argue, are essentially due to their interactions with dislocations. The SmA $\rightarrow$ N phase transition has been the object of many investigations (for a review, see [3]). The compression modulus B tends towards a value equal to or slightly different from zero, according to the author, see *e.g.*, [4-7]; its variation is noticeable in a large temperature range (more than half a degree in the compounds that we have investigated). Notice that in this range K_1 (the splay modulus) stays practically constant. The question of $\overline{K}$ (the saddle-splay modulus) has been little investigated yet, either theoretically or experimentally (see [8] for the nematic phase); the results that follow have been interpreted by assuming that $\overline{K}$ too stays practically constant. K_2 **(the twist modulus) is infinite in layered media as long as the director remains along the layer normal (which might be infirmed very close to the nematic transition).**

Let us now recall some defect features of the SmA phase. These defects are of two types, focal conic domains (which are especial types of disclinations) and dislocations:

focal conic domains (FCDs): the layers are parallel, so that there is no strain energy but only curvature energy. The normals to the layers envelop two focal surfaces on which the curvature is infinite (the energy diverges). The focal surfaces are degenerate into lines in order to minimize this large curvature energy. These lines are necessarily two confocal conics, an ellipse and a hyperbola, observable by optical microscopy [9-13]. The layers are folded along *Dupin cyclides*, surfaces that have the topology of tori. And indeed the simplest geometric case is when the ellipse E is degenerate into a circle – the confocal hyperbola H being degenerate into a straight line perpendicular to the plane of the circle and going through its centre. In this case the layers are nested tori, restricted in fact to those parts of the tori that have negative Gaussian curvature $G=\sigma_1\sigma_2$. The $G < 0$ case is indeed the most usual case met experimentally in generic Dupin cyclides, see [14,15]. We shall not consider in the sequel the situations where the layers are restricted to those parts that have positive Gaussian curvature; and as a matter of fact the mixed case is not observed. In the toric case just alluded, the focal conic *domain* is the region of space occupied by those nested layers restricted to their $G < 0$ parts; it is bound by a cylinder parallel to H and whose cross section is E. In the generic case, the region of space where the layers have $G < 0$ is bound by two half-cylinders of revolution, that

meet on the ellipse, and whose generatrices are parallel to the hyperbola asymptotes, Fig. 1a. This is the picture of an ideal, *complete*, FCD. Fig. 1b illustrates a case where $G < 0$ and $G > 0$ regions are visible in the same FCD; it does not correspond to any situation met in practice. Models for ideal, *incomplete* FCDs are shown farther ahead (Fig. 9a and 9b). The important question how FCDs are packed in space [10, 11] will be approached, but only incidentally.

The curvature energy f_{FCD} of a complete, ideal, focal conic domain depends on K_1 and $\overline{K}$:

$$f_{\mathrm{FCD}} = f_{\mathrm{bulk}} + f_{\mathrm{core}} = 4\pi\, a(1-e^2)\mathbf{K}(e^2)[K_1 \ln\frac{2b}{\xi} - 2K_1 - \overline{K}] + f_{\mathrm{core}} \qquad (1)$$

where a is the semi-major axis of the ellipse, b the semi-minor axis, e the eccentricity and $\mathbf{K}(e^2)$ the complete elliptic integral of the first species [14]. It has been advanced that the energy f_{strain} attached to the thickness variation of the layers is negligible compared to f_{FCD} [11,14] ; see also [13] for another approach. Very little is known about the core contribution f_{core}, but it is usually assumed that it scales as aK_1 . Thus, at a and e constant, the FCD total energy does not vary significantly in the domain of temperature under investigation, if our assumptions about the temperature variation of K_1 and $\overline{K}$ turn to be true.

screw dislocation lines and edge dislocation lines: their unit length line energies can be written:

$$f_{\mathrm{s}} = \frac{1}{128}\frac{B b_{\mathrm{disl}}^4}{r_{c,screw}^2} + f_{\mathrm{core}}, \qquad f_{\mathrm{e}} = \frac{1}{2}\sqrt{K_1 B}\,\frac{b_{\mathrm{disl}}^2}{r_{c,edge}} + f_{\mathrm{core}}, \qquad (2)$$

where $b_{\mathrm{disl}} = n\, d_0$ is the dislocation Burgers vector (d_0 is the layer thickness) and r_c is the core radius. It is visible that the elastic contributions (the off-core terms in Eq. 2) decrease when T gets closer to T_{AN}, because B decreases whereas the temperature changes of the core energies can be neglected or even decrease –indeed in a naïve model inspired by the solid-liquid transition, these energies are of order $k_{\mathrm{B}}(\mathrm{T}_{\mathrm{AN}} - \mathrm{T})\frac{\pi r_c^2}{\delta^2 d_0}$ per unit length of dislocation line, *i.e.* small; $\delta^2 d_0$ is the volume occupied by a molecule, and r_c is microscopic, practically constant (of order δ for a screw dislocation, d_0 for an edge dislocation). The decrease of B, as already stated, is effective on a large temperature range before the transition, probably larger than $1°C$, see [4,6]. The core radii scale as the correlation lengths very close to the transition, but this region is of no interest to us.

Comments on the experimental conditions

The FCDs are stable and immobile in the lower part of the temperature range we have investigated; they however quite often display variations to their ideal shape. The transformations of the FCDs, when approaching the transition, are visible with a simple optical microscopy set up. They appear as rather sudden phenomena, about half a degree below T_{AN}, at a temperature T^* that depends slightly on the boundary conditions. **Our observations relate to *thermotropic* compounds, two belonging to the cyanobiphenyl series, 8CB and 9CB. We also noticed that FCD texture of the 10CB compound does not display any conspicuous modifications when T increases, but this chemical does not have a nematic phase; the transition is direct to the isotropic phase. This is in contrast with the other compounds, that have a SmA → N transition.** In these latter cases, either the FCDs

disappear by shrinking before the phase transition, or the ellipse and the hyperbola transform into disclinations in the nematic phase; the first situation occurs usually for small and medium size (tens of microns in diameter) slowly FCDs heated (heating rate lower than 0.1°C/min), the second one occurs for large (hundred of microns and more in diameter) FCDs, when they are brought to the transition under faster heating (this linear scaling is conditional, depending on the heating rate: at a high heating rate of several degrees per minute, even small FCDs have no time to shrink). When cooling down from the nematic phase, the FCD texture in 8CB and 9CB usually does not display ideal FCDs. Instead FCD fragments grow, join and form focal domains, which in many cases are not ideal. The double helical objects described in [16], which are splitting modes of giant screw dislocations, are obtained this way. **These *imperfect* FCDs (iFCD) can be quenched to lower temperatures where they stabilize because of a much reduced mobility (high viscosity).** The boundary conditions play an important role in the definition of the final texture.

We believe that the transformations of the FCD texture in 8CB, 9CB when approaching the nematic phase, as well as the formation of iFCDs when coming from above, are due to the interaction of the FCDs with dislocations. Dislocations are generally not visible by optical microscopy, except when their Burgers vector is large (micron size), which situation occurs for edge dislocations clustering into oily streaks [9-11] or screw dislocations split into two k=1/2 disclinations [16, 17]. We argue here that the presence of numerous dislocations can be revealed via their distorting action on the FCDs, which are visible.

II. GEOMETRIC RULES FOR IDEAL FOCAL CONIC DOMAINS

Essential for a better understanding of the modifications suffered by FCDs when interacting with dislocations are the following properties, that characterize them when they are in an *ideal* state.

(a)- Projected orthogonally upon a plane, along any direction, the ellipse E and the hyperbola H cross at right angles, Fig. 2a. This is a particular case of Darboux's theorem [18], which states that if a congruence of straight lines is orthogonal to a set of parallel surfaces, the two focal surfaces Σ_1 and Σ_2 (that this congruence generically envelops) are such that the planes tangent to Σ_1 and Σ_2 at the contact points M_1 and M_2 of any line Δ of the congruence are orthogonal. This is the reason why the projections of the ellipse E and the hyperbola H belonging to the same FCD look orthogonal. Here the straight line Δ is a normal to the Dupin cyclides, and indicates the average direction of the molecules. Darboux's theorem is empirically satisfied by a number of FCDs, which in that sense are ideal FCDs; when it is not, (see Fig. 2b), it implies that the FCD in question is geometrically interacting with other defects, as we shall discuss in the sequel.

(b)- The inner layers of an *isolated complete* FCD can be continued outside the FCD by planar layers perpendicular to the asymptotes (this is obvious from Fig 1a), which can form two sets of parallel planes meeting on the plane of the ellipse, along a direction parallel to the minor axis of the ellipse, at an angle ω. The plane of the ellipse is therefore a tilt grain boundary. In a solid crystal, a tilt grain boundary is usually split into edge dislocations whose Burgers vectors are perpendicular to its plane. The same is of course possible for a tilt grain boundary in a layered medium. One expects that some of those dislocations meet the ellipse. As a matter of fact, the ellipse of an isolated FCD is the termination of a set of dislocations whose total Burgers vector $b_{\mathrm{disl}} = 4ae = 4c$, as explained below.

(c)- Two neighboring ideal FCDs whose ellipses are in the same plane and tangent at some point M are in contact along at least one line segment joining M to a point P at which the two hyperbolae intersect. **This geometry, frequently observed, is a particular realization of the law of corresponding cones [9-11], a geometrical property that rules the way FCDs pack in space.** A tilt grain boundary whose angle of misorientation ω is neither too small nor too large is usually made of a FCD packing such that the ellipses belong to the grain boundary, have a constant eccentricity $e = \sin\frac{\omega}{2}$, the asymptotes of the hyperbolae being parallel [19], see Fig. 3. And indeed the free interstices of the packing of ellipses in the plane of the grain boundary are filled with dislocations [19]. There is a relation of equivalence between dislocations and focal conic domains [20, 21].

III. KINKS ON DISCLINATIONS

A. Wedge and twist disclinations. FCD confocal conics are disclinations.

Disclinations are typical line defects in a medium endowed with a *director* order parameter [22]. One distinguishes *wedge* disclinations, whose rotation vector $\boldsymbol{\Omega}$ is along the disclination line, and *twist* disclinations, whose rotation vector $\boldsymbol{\Omega}$ is orthogonal to the disclination line. As shown in [9, 10], there are necessarily dislocations attached to a line segment of twist character. Let us remind that the focal lines of a FCD, are, by nature, disclinations.

(a)- The hyperbola is a disclination of strength $k = 1$, whose rotation vector ($\boldsymbol{\Omega} = 2\pi\mathbf{t}$) varies in direction (not in length) all along the hyperbola: at each point of the hyperbola it is parallel to the tangent $\mathbf{t}$ at this point. The layer geometry is axial-symmetric in the vicinity of the hyperbola. Insofar as it is a disclination, the hyperbola is of wedge character; there are no attached dislocations.

(b)- If the full cyclides are considered, as in Fig. 1b, the layers that surround the ellipse are axial-symmetric about the tangent to the ellipse; the ellipse appears also as a $k = 1$ wedge line. But, if one restricts to the inner $G < 0$ layers of the complete FCD, supplemented by the outer planar layers, the ellipse appears as a disclination of strength $k = \frac{1}{2}$, whose rotation vector ($\boldsymbol{\Omega} = \pi\mathbf{t}$) varies (in direction but not in length) all along the ellipse; $\mathbf{t}$ is in the plane of the ellipse and tangent to the layer inside the ellipse, Fig. 4. This disclination is of mixed character; the attached dislocations are precisely those that form the tilt boundary [15, 19, 23] whose existence has been established above; see below for more details.

B. Kinks, generic properties.

Modifications to the twist/wedge character of a disclination can be achieved in the generic case by attaching/detaching new dislocations to the line. Such operations modify the shape of the line, by the introduction of *kinks*, Fig. 5. For instance, in order to attach at some point A on a wedge line L a set of dislocations of total Burgers vector b_{disl}, one has to introduce a kink **AB**, with a component perpendicular to L, (*i.e.* a segment **AB** having a twist component), such that

$$\boldsymbol{b}_{disl} = 2\sin\frac{\Omega}{2}\mathbf{t}\times\mathbf{AB}, \tag{3}$$

where $\mathbf{t}$ is an unit vector tangent to the line and $\boldsymbol{\Omega}$ ($\boldsymbol{\Omega}=\Omega\mathbf{t}$) is the rotation invariant carried by the disclination; see [11, 23] and the Appendix for a demonstration of Eq. (3). In practice lines of interest are of strength $|k|=\frac{1}{2}$, $|\boldsymbol{\Omega}|=\pi$. Reciprocally, the presence of a kink reveals the presence of dislocations attached to the line. The above picture of a kink says nothing about the nature (edge or screw) of the attached dislocations, and the way they relax and disperse through space about the disclination line. The line flexibility, *i.e.* the main property at work when the medium is deformed, elastically or by flow, takes its origin here, in this interplay of the disclination line with dislocations.

A kink can be infinitesimally small;

$$d\boldsymbol{b}_{disl} = 2\sin\frac{\Omega}{2}\mathbf{t}\times d\boldsymbol{s}, \tag{4}$$

where $d\boldsymbol{s}$ is an infinitesimal element along the line [23]. A density of infinitesimally small kinks modifies the curvature of the line. A dislocation attached to an infinitesimally small kink has an infinitesimally small Burgers vector; a dislocation attached to a finite kink may have a finite Burgers vector, as we see now.

C. Kinks in a SmA

Let us now consider in more detail the geometry of the attachment of dislocations to a focal line in a FCD. We first state some general properties, and then consider separately the case of the ellipse and the case of the hyperbola.

Again, the dislocations emanating from the kink have to belong to one of the two following categories: they are either dislocations with infinitesimal Burgers vectors whose directions are parallel to the layer dislocations of the layer stacking, or with Burgers vectors $|\boldsymbol{b}_{disl}|=nd_0$ perpendicular to the layer (these are the usual SmA quantified dislocations). Note that in both cases the Burgers vectors are translation symmetry vectors; they are *perfect* Burgers vectors in the sense of the Volterra process. We consider them successively.

Infinitesimal Burgers vectors relate to dislocation densities that relax by the effect of viscosity; they affect the curvature of the layers and consequently, as alluded just above, they also affect their thickness, since the layers have to keep in contact. We shall not expatiate on such defects, which are not relevant to our subject. **Just note that the theory has been developed for solids since long, (see [24] for a general review) and is related to the concept of densities of infinitesimal dislocations in nematics and cholesterics introduced first in [23]; see also [11, 17].** An essential point worth emphasizing is that a continuous density of infinitesimal dislocations can be attended by a strainless, elastically relaxed, state. In our case, this would correspond to a state where the layers have curvature and keep parallel. Continuous dislocations with Burgers vectors parallel to the layers do not introduce any kind of singularity of the SmA order parameter. Eq. (4) indicates that the related kink $d\boldsymbol{s}$ and that $\mathbf{t}$ are both perpendicular to $d\boldsymbol{b}_{disl}$, which condition does not specify any special direction for $d\boldsymbol{s}$.

Finite Burgers vectors: this case is better represented by Eq. (3), because the Burgers vector and the kink

AB are both finite. **AB** and **t** have both to be in a plane tangent to the local layer. To an elementary dislocation $|\boldsymbol{b}_{disl}| = d_0$ corresponds an elementary kink. An elementary kink is microscopic (with $|k| = \frac{1}{2}$, $|\Omega| = \pi$, one has AB = $2d_0$); one can thus possibly have a density of such elementary kinks, rendering the line curved when observed at a mesoscopic scale. This does not exclude the possibility that infinitesimally small dislocations are attached to finite kinks.

Simple as they look, the application of these criteria requires however some care.

D. Quantified Burgers vectors attached to an ellipse.

Fig. 4 is a schematic view of the properties of an ellipse, belonging to an ideal FCD, in relation to its $k = \frac{1}{2}$ disclination character. The layer geometry is different inside and outside the ellipse. *Inside*, the Dupin cyclide layers intersect the plane of the ellipse *perpendicularly*. ***Outside*, the layers are planar and *perpendicular* to the asymptotic directions.** The change of geometry between the inside and the outside is achieved by a rotation of the layers about the local rotation vector $\boldsymbol{\Omega}=\Omega\mathbf{t}$; $\boldsymbol{\Omega}$ is parallel to the layers (inside and outside) and is along the intersection of the layers with the plane of the ellipse, inside.

The layer at M (M being a running point on the ellipse) is indeed folded inside about the local **t** direction, is singular at M (it is a conical point), and extends outside along a fold made of two half planes symmetrical with respect the ellipse plane, each perpendicular to one or the other of the two asymptotic directions of the confocal hyperbola, and thereby making an angle $\omega=2\sin^{-1}e$ about a direction parallel to the minor axis of the ellipse (see [11], chapter 10). **The ellipse plane outside the ellipse is therefore a tilt boundary of misorientation angle ω, which can be accommodated by edge dislocations of Burgers vectors multiple of d_0, perpendicular to the plane of the tilt boundary, *i.e.* the plane of the ellipse outside.** There is one such dislocation $|\boldsymbol{b}_{disl}| = 2d_0$ per layer counted inside the ellipse. These results are similar to those obtained in section II; they also justify the choice of $\boldsymbol{\Omega}$ we have done for the disclination rotation along the ellipse.

The same result can be obtained by using Eq. (4). Let us parameterize the ellipse in polar coordinates with the origin at the physical focus, Fig. 6.

$$r = \frac{p}{1 + e\cos\phi}, \tag{5}$$

where $p = \frac{b^2}{a}$ and ϕ is the polar angle. Applying Eq. (4), one then finds that the $k = \frac{1}{2}$ ellipse disclination has an attached Burgers vector density

$$db_{disl} = 2dr, \tag{6}$$

The total Burgers vector attached to the ellipse is $\int_{\phi=0}^{\phi=\pi} db_{disl} = 4c$, as indicated above. If one takes $dr = d_0$, – an approximation which makes sense (up to second order), since d_0 is so small compared to the size a of the ellipse – it is visible that the points $\mathbf{M}\{r,\phi\}$ and $\mathbf{N}\{r+dr,\phi+d\phi\}$ are on two parallel smectic layers at a distance d_0.

Notice that the density of dislocations is constant if measured along the major axis: $\frac{db_{disl}}{dx} = -2e$. There are no dislocations attached to the singular circle of a toric FCD, as the eccentricity e vanishes. An ellipse can be thought of as a circle kinked at the layer scale.

IV. KINKED FOCAL CONIC DOMAINS

A. Frequent geometries for a kinked ellipse.

The kinking of the ellipse takes different geometries, whether the dislocations at stake are located inside the ellipse (where $b_{disl} = nd_0$ is in the plane of the ellipse, the layers being perpendicular to this plane) or outside (where $b_{disl} = nd_0$ is perpendicular to the plane of the ellipse).

***Outside the FCD*; in that case the kinking of the ellipse is in its plane. This in-plane kinked ellipse, we call it a Mouse (Fig. 7). If the dislocation lines attached to the ellipse disperse away *outside* the focal conic domain, *i.e.* in a region of space where the layers are in the plane of the ellipse, $\mathbf{t}$, which varies in direction all along the ellipse, is in this plane.** Applying Eq. (3), it appears that the kinks have to be in the plane of the ellipse. This configuration has been observed, in a situation where the kinks are so small and have such a high density that the kinked ellipse appears to be continuous, but its shape departs considerably from a 'perfect' ellipse; **it is smoothly distorted by the in-plane kinks: this is the reason why we use the term of Mouse (Fig. 7a).** Fig. 7b provides a model for such kinks, (which always go by pairs), drawn here at a scale which has no relation with the real scale. The photograph of Fig. 7a is taken from the rim of a free-standing film, in a region where the thickness of the film is quickly changing, and the wedge angle $\omega(r)$ between the opposite free boundaries varies monotonically. The anchoring conditions are homeotropic; there is therefore a tilt boundary in the mid-plane of the film, but with a variable misorientation angle. **The Mouse is in this mid-plane; the extra dislocations attached to the kinks (edge dislocations in the mid-plane) relax the variation of ω by contributing to the modification of the density $d\,b_{disl}/ds$ of dislocations in this plane; see [2] for a more detailed account.**

***Inside the FCD*; in that case the kinking of the ellipse brings a part of it out its plane.** This off-plane kinked ellipse, we call it a Turtle (Fig. 8). The layers rotate about $\mathbf{t}$ by an angle of π; hence they become perpendicular to the plane of the ellipse, *inside* the FCD. Therefore the dislocations that disperse away inside are attached to kinks that are perpendicular to the plane of the ellipse, on average. A pair of elementary kinks (not at scale at all in the figure), symmetric with respect to the major axis, can be linked by a unique dislocation (Fig. 8b). Our observations (Fig. 8a) indicate the existence of another mode of kinking, with screw dislocation segments joining the kinks (of macroscopic size) to the hyperbola. There is no kink on the hyperbola, because the two screw segments are of opposite signs, if both oriented *e.g.* toward the hyperbola; they therefore induce opposite kinks. We call such a departure from the perfect ellipse, distorted by off-plane kinks, a 'Turtle'. One can eventually imagine elementary kinks of the sort, all of the same sign, having a high density on the ellipse and continuously tilting its plane. Such tilted ellipses have been observed in 8CB and 9CB [1]. The situation observed in Fig. 8a results from the presence of a quasi planar *pretilted* anchoring. A unique direction of pretilt is in conflict with the presence of an entire ellipse

parallel to the boundary in its close vicinity; hence opposite displacements of different parts of the ellipse along the vertical direction, to the point that one part gets off the boundary, and is virtual~~; see [2] for a more detailed account of this geometry and other geometries implying different kink types~~. Fig. 8c illustrates a double-kinked ellipse of a Turtle type observed from the side in a thick 8OCB sample ($\approx 100\mu m$).

B. On the origin of deviations from Darboux's theorem.

The just alluded kinking processes can bring large deviations to Darboux's law; reciprocally it is clear that the deviations from Darboux's law mean a modification of the shape of the ideal FCD conics, *i.e.* the presence of kinks (at the scale of the layers, since they are not visible with the optical microscope) and of their attached dislocations. These dislocations necessarily disperse through the medium, outside and/or inside the FCD. Infinitesimal dislocations, if alone, would result, as stated above, in an extra curvature of the layers; two cases arise: **either the deformed layers keep parallel, hence the layer normals keep straight,** and one gets eventually a new ideal FCD, or there is a deviation to straightness of the layer normals, and consequently a layer thickness variation (this case falls within the province of the Kroener's dislocation densities [24]), *i.e.* a process of high energy if not relaxed, at least in part, by finite edge dislocations. It suffices then to consider only those latter. The edge components of the attached dislocations that are dispersed *inside* the FCD break the parallelism of the inside layers. The congruence of the layer normals is thus no longer a set of straight lines. This is another way of explaining the variation to Darboux's theorem. This could have been stated from the start: *edge dislocation densities break Darboux's theorem, because they break layer parallelism.* But this statement comprehends deviations to Darboux's theorem that are more general than those where the focal manifolds are degenerate to lines. The focal manifolds of a congruence of curved normals are generically 2D surfaces, not lines. **We see that the fact that these surfaces are degenerate into lines comes from ~~the fact that~~ the *attachment* of the dislocations in question ~~are~~ to the original focal lines.** To conclude, the occurrence of deviations to Darboux's theorem for a set of focal *lines* means that the conics are (densely) kinked and dislocations attached to those kinks.

C. The kinked (split) hyperbola.

The shape of the layers is cylindrical about the central zone of the hyperbola, near its apex (which is also the physical focus of the ellipse). But the layers are practically perpendicular to the hyperbola at a distance from the plane of the ellipse of order a; the wedge disclination smoothly vanishes far from the ellipse plane. In between, the layers display cusps, the lesser pronounced the more distant from the ellipse. Hyperbolae are lines of easy coalescence of screw dislocations, as observed long ago [25].

The presence of kinks on the hyperbola is a delicate matter; because it is a $k = 1$ wedge disclination ($\Omega = 2\pi$.), Eq. (3) and (4) do not apply directly. A way of solving the question is to consider that the line is made of two $k = \frac{1}{2}$ lines, indicating that dislocations with total Burgers vectors twice as large can attach to a kink of the same size as in the $k = \frac{1}{2}$ case.

Another situation is worth considering. In incomplete focal domains of the type represented Fig. 9b (called *fragmented* domains), the hyperbola belongs to the boundary of the domain. It is then no longer a $k = 1$ disclination

but a $k = \frac{1}{2}$ disclination, as if it were split all along its length. **Fragmented FCDs, noted fFCD for short, already recognized by G. Friedel [10], are easily obtained in a confined sample with degenerate boundary conditions. A fFCD is bound by a segment of the ellipse and by a segment of the hyperbola, and four fragments of cones of revolution. Thus both segments are $k = \frac{1}{2}$ disclination line segments.**

As a consequence, fFCDs are generally aligned, attached by the ends of the disclination segments, such attachments being required by the conservation of the disclination strength. But observe that a hyperbola H (resp. an ellipse E) can be attached indifferently either to another H (resp. an E) or to an E (resp. a H).

One can imagine that the ellipse E_1 of a FCD_1 is attached to H_2 of a FCD_2, while the hyperbola H_1 of the FCD_1 is attached to E_2 of the FCD_2. Such a set of line segments attached by their extremities is topologically equivalent to a double helix. This geometry, with sequences of the …HEHEH… type, was observed long ago by C. E. Williams [16] at the N → Sm transition; it is at the origin of helical giant screw dislocations. **Fig. 10a shows an elementary fFCD having the shape of a tetrahedron; the disclination segments are of opposite 'concavities', which implies that the ellipse segment is chosen close to the physical focus. Such tetrahedra are documented in [10]. Fig 10b shows the abuting of several tetrahedra, which are no longer perfect fFCD volumes.**

Let us also mention the observation, also reported in [1], of a mobile kink (several microns long) perpendicular to the $k = \frac{1}{2}$ hyperbola of a fFCD, moving in the direction of the physical focus, but nucleated far from it, at a distance large compared to a. There is no doubt that dislocations, dragged along the hyperbola, are attached to this mobile kink; their Burgers vectors, that are perpendicular to the layers, are practically parallel to the asymptotic direction of the hyperbola, at a distance from the ellipse plane, which indicates that they are of screw character. This might be an indication of a mechanism by which screw dislocations align along a (split) hyperbola.

D. Focal Conic Domains at the Sm → N transition

FCDs that are immersed in the bulk (they are of the type represented Fig. 9a, and generally gather into tilt boundaries) disappear rather suddenly about $0.5°C$ before the transition, by an **instability** mechanism that might imply a sudden multiplication of dislocations. The spontaneous multiplication of screw dislocations close to the SmA→ N transition is a well-documented fact in *lyotropic* systems [26-27], which inclines us to believe that the phenomenon of spontaneous multiplication of dislocations (screw but also edge) is very general. The capture of free edge dislocations by the ellipse modifies its geometric features *e* and *a*, **Fig. 11.** Free dislocations of the same (*resp*. opposite) sign as the dislocations attached to the ellipse, if captured, would increase (*resp*. decrease) its size ($2a \rightarrow 2a + b_{disl}$), either at *e* constant (then the asymptotic directions stay constant), or not. **Boundary conditions play a dominant role in this relaxation process.** Notice that, after a possible increase in size, the ellipses eventually always decrease in size when the temperature increases, the smallest ellipses disappearing first. For the ellipses belonging to a grain boundary, this implies that the boundary area occupied by dislocations (the so-called residual boundary) increases with temperature. This is in agreement with the model developed in [19], which relates

the residual boundary to the material constants; in particular a decrease of the compression modulus B must result in an increase of the residual area.

V. CONCLUSION

This paper investigates from a theoretical point of view some features of the FCD transformations that have been observed, in the smectic phase, when approaching the nematic phase. These very spectacular phenomena happen in a large temperature domain ($\Delta T = T_{AN} - T^* \approx$ half a degree in 8CB, which is the chemical we used for quantitative observations; the other compounds yield qualitatively equivalent results) in which it is believed that the variations of the material constant B are large enough to allow significant variations of the dislocation line energy and the multiplication of fresh dislocations. At the same time K_1 and also $\overline{K}$ (as we assume) do not vary in comparable proportion, so that the energy of focal conic domains is not appreciably changed.

We have tried to discuss the general principles at the origin of these transformations that are due to the direct interaction between FCDs and finite Burgers vector dislocations. There is no doubt that infinitesimally small Burgers vector dislocations are also playing a role, in particular in the phenomena of viscous relaxation [11,28], but this is not discussed. The general principles that we advance are geometrical and topological in essence. The mechanisms that obey these principles seem to be plenty, depending in particular on the boundary conditions and the precise FCD texture. The examples we have given are few, and are chosen for the sake of illustration. ~~A description of several more observed transformations, interpreted in the same terms, will be given somewhere else.~~

The SmA $\rightarrow$ N transition is one of the most debated liquid crystal phase transitions [3, 29-31]. This is not the place to enter into the detail of this debate, inasmuch as our results, even if they stress the importance of defect interplays in the critical region, are not directly related to the very proximity of the transition, which has been examined by several authors with great accuracy (*e.g.* [7]).

The question that is at stake is rather why the interactions occur at temperatures definitively lower than T_{AN} and result in an instability of the FCDs. **More details about the instability will be given in a forthcoming publication ~~[2].~~**

VI. APPENDIX

We envision a curved disclination line $\mathtt{L}$, carrying a rotation vector $\boldsymbol{\Omega}$ constant in length and in direction. Let P be a point on the cut surface bound by $\mathtt{L}$.

We first assume that $\boldsymbol{\Omega}$ is attached to some well-defined point $\mathbf{O}$, **Fig. 12.** The relative displacement of the two lips of the cut surface at $\mathbf{P}$ is

$$\boldsymbol{d}_{\mathbf{P}}(\mathbf{O}) = \boldsymbol{\Omega} \times \mathbf{OP} \qquad (7)$$

which is large on the line $\mathtt{L}$ if $\mathbf{P}$ is taken at some point $\mathbf{M}$ on $\mathtt{L}$. Consequently in the generic case $\mathtt{L}$ ($\mathbf{0}$, $\boldsymbol{\Omega}$) has a very large core singularity, thus large accompanying stresses and a large core energy. On the other hand the cut

surface displacement vanishes at $\mathbf{M}$ if $\boldsymbol{\Omega}$ is attached to L at $\mathbf{M}$, but then it does not vanish at $\mathbf{N} = \mathbf{M} + \mathrm{d}\mathbf{M}$. There is still a large core singularity along L, except at $\mathbf{M}$. The Volterra process, when applied in its standard form, does not provide a solution to the construction of a curved disclination with well relaxed stresses.

An extended conception of the Volterra process solves the problem. Assume that there is a copy of the rotation vector $\boldsymbol{\Omega}$ attached to all the points of L, and consider the effect of such rotation vectors on a point $\mathbf{P}$ belonging to the cut surface ~~of all these $\boldsymbol{\Omega}$'s~~. We have, for each other $\mathbf{M}$ belonging to L, ~~another~~ a value of the relative displacement of the lips of the cut surface which can be written:

$$\boldsymbol{d}_{\mathbf{P}}(\mathbf{M}) = \boldsymbol{\Omega} \times \mathbf{MP} \qquad \textbf{(8)}$$

Each M on L yields another value of the relative displacement at the same point P of the cut surface, but this difficulty can be solved by the introduction of a set of *infinitesimal* dislocations attached to the disclination line all along L, Fig. 13. Indeed, let $\mathbf{M}$ and $\mathbf{N} = \mathbf{M} + \mathrm{d}\mathbf{M}$ be two infinitesimally close points on L. We have:

$$\boldsymbol{d}_{\mathbf{P}}(\mathbf{M} + \mathrm{d}\mathbf{M}) - \boldsymbol{d}_{\mathbf{P}}(\mathbf{M}) = \boldsymbol{\Omega} \times \mathrm{d}\mathbf{M} \qquad (9)$$

which is independent of $\mathbf{P}$. The quantity $\boldsymbol{db}(\mathbf{M}) = \boldsymbol{\Omega} \times \mathrm{d}\mathbf{M}$ is the infinitesimal Burgers vector of the infinitesimal dislocation attached to L at point $\mathbf{M}$ [23].

The above equations are established for a small angle of rotation vector $|\boldsymbol{\Omega}|$. In the general case $\boldsymbol{\Omega}$ has to be replaced by $\frac{1}{2}\sin\frac{\Omega}{2}\mathbf{t}$, where $\boldsymbol{\Omega} = \Omega\,\mathbf{t}$.

****

ACKNOWLEDGMENTS. We acknowledge fruitful discussions with Dr V. Dmitrienko and Pr. J. Friedel. We are grateful to Dr. J.-F. Blach for providing us with glass plates treated for special anchoring conditions.

REFERENCES

[1] C. Meyer and M. Kleman, ILCC20, Mol. Cryst. Liq. Cryst., **437**, 111[1355] (2005).

[2] Yu. A. Nastishin, C. Meyer and M. Kleman, in preparation.

[3] P. G. De Gennes and J. Prost, *The Physics of Liquid Crystals*, second edition, Clarendon Press (1993).

[4] M. Benzekri, T. Claverie, J.-P. Marcerou, and J.-C. Rouillon, Phys. Rev. Lett. **68**, 16 (1992).

[5] D. Rogez, D. Collin and P. Martinoty, Eur. Phys. J. **E14**, 43(2004).

[6] F. Beaubois, T. Claverie, J.-P. Marcerou, J.-C. Rouillon, and H.-T. Nguyen, C.W. Garland and H. Haga, Phys. Rev. **E56**, 5 (1997).

[7] A. Yethiraj, J. Bechhoefer, Phys. Rev. Lett. **84**, 16 (2000).

[8] G. Barbero and V. M. Pergamenshchik, Phys. Rev. **E66** 051706 (2002).

[9] G. Friedel et F. Grandjean, Bull. Soc. Fr. Minér. **33**, 192, 409 (1910).

[10] G. Friedel, Ann. Phys. (Paris) **18**, 273 (1922).

[11] M. Kleman and O. D. Lavrentovich, *Soft Matter Physics. An Introduction*, Springer N.Y. (2003).

[12] C. E. Williams, *Défauts de structure dans les smectiques A*, PhD Thesis, Orsay, France (1976).

[13] J-B. Fournier and G. Durand, J. Phys. II France **1**, 845 (1991).

[14] M. Kleman and O. D. Lavrentovich, Phys. Rev. **E61**, 1574 (2000).

[15] P. Boltenhagen, O. Lavrentovich and M. Kléman, Phys. Rev. **A46**, 1743 (1992).

[16] C.E. Williams, Philos. Mag. **32**, 313 (1975).

[17] M. Kleman, O. D. Lavrentovich and Yu. A. Nastishin, in *Dislocations in Solids*, F. R. N. Nabarro and J. P. Hirth, eds, North-Holland, Amsterdam vol. **12**, 147 (2004).

[18] G. Darboux, *Leçons sur la théorie générale des surfaces*, seconde partie, Gauthier–Villars, Paris (1914).

[19] M. Kleman and O. D. Lavrentovich, Eur. Phys. J. **E2**, 47 (2000).

[20] L. Bourdon, M. Kléman and J. Sommeria, J. de Physique **43**, 77 (1982).

[21] P. Boltenhagen, O. D. Lavrentovich and M. Kléman, J. Phys. II France **1**, 1233 (1991).

[22] F. C. Frank, Discuss. Faraday Soc. **25**, 19 (1958).

[23] J. Friedel and M. Kléman, J. de Phys. **30**, C4:43 (1969).

[24] E. Kroener, in *Physics of Defects*, Les Houches 1980 Session XXXV (eds. R. Balian, M. Kléman and J.P. Poirier), North-Holland, Amsterdam, (1981).

[25] C. E. Williams and M. Kléman, Philos. Mag. **33**, 213 (1976).

[26] M. Allain and J.-M. diMeglio, Mol. Cryst. Liq. Cryst. **124**, 115 (1985), Europhys. Lett. **2**, 597 (1986).

[27] O. Dhez, S. König, D. Roux, F. Nallet and O. Diat, Eur. Phys. J. **E3**, 377 (2000).

[28] J. Friedel, private communication.

[29] J. Toner and D. Nelson, Phys. Rev. **B24**, 363 (1981).

[30] J. Toner, Phys. Rev. B26, **1** (1982).

[31] W. Helfrich, J. de Physique **39**, 1199 (1978).

Fig. 1. (Color on line) a)- Complete FCD with negative Gaussian curvature Dupin cyclides, sitting inside two cylinders of revolution meeting on the ellipse. The cyclides cross the ellipse plane at right angles; their intersections with the ellipse and the hyperbola, when they exist, are conical points. b)- Dupin cyclide fragments with positive and negative Gaussian curvature, so chosen that the ellipse is still singular but the hyperbola has no physical realization. A FCD with positive and negative Gaussian curvature both present, the hyperbola singular and ellipse not physically realized, is illustrated in [11].

Fig. 2. (Color on line) In a ideal FCD the ellipse and the hyperbola project orthogonally along two conics which intersect at right angles. (Photographs longer edges ≈ 200μm): a)- 8OCB, between two untreated glass substrates, sample thickness approx. 200μm, 7°C below the transition, polarized light microscopy; Darboux's theorem obeyed; the FCDs with parallel hyperbola asymptotes form a tilt boundary of the type schematised Fig. 3; b)- 8CB, 0.5°C below the transition, polarized light microscopy; Darboux's theorem disobeyed as demonstrated in the lower photograph: the solid lines are tangent to the disclinations and the dashed lines perpendicular to them; a very visible deviation from Darboux's theorem is encircled on the upper photograph.

Fig. 3. (Color on line) Tilt boundary split into FCDs. TOP: schematic, adapted from [11]; BOTTOM: 8CB, polarized light microscopy; the tilt boundary is seen edge-on; edge of the photograph ≈ 100μm long.

Fig. 4. F, the physical focus, is the centre of the (circular) intersections of the layers with the plane of the ellipse, inside the ellipse; $\vec{t}$ is a unit vector along the local rotation vector; the k = 1/2 disclination ellipse is of mixed (twist-wedge) character all along, except at the ends of the major axis, where it is wedge.

Fig. 5. Kink on a wedge disclination line, see text

Fig. 6. The ellipse in polar coordinates. The radius of curvature of the circle centred in the focus F and tangent to the apex is a - c, which is smaller than the radius of curvature b^2/a of the ellipse at the apex. This circle is thus entirely inside the ellipse. All the circles and the arcs of circles of the figure are centered in F. They figure intersections of the smectic layers with the plane of the ellipse.

Fig. 7. Double kinks with dislocations *outside* the FCD; a)- Mouse patterns in 8CB, free standing film, rim region; the thickness decreases downward; longer edge of the photograph ≈ 200μm; b)- model.

Fig. 8. Views of a double kink with a dislocation *inside* the FCD; longer edge of the photograph ≈ 200μm; a)- turtle patterns in 8CB, demonstrating that the ellipses are divided into two parts not located at the same level, the screw dislocations attached to the kinks are visible; b)- model of a double kink linked by a unique dislocation located inside the FCD; c)- a double kinked ellipse (kinks are indicated by arrows) of the turtle type observed from the side (8CB in a gap of thickness ≈ 100μm between two untreated glass substrates).

Fig. 9. (Color on line) Incomplete FCDs. a)- FCD bound by two cones of revolution meeting on the ellipse, with apices at the terminations of the hyperbola segment; b)- A hyperbola-split fragmented FCD (fFCD). The fFCD is bound by i) two fragments of cones of revolution with apices at the terminations of the hyperbola segment and limited to the ellipse segment, ii) two fragments of cones of revolution with apices at the terminations of the ellipse segment and limited to the hyperbola segment. The director field on the boundaries is indicated, not the cyclide intersections with these boundaries.

Fig. 10. (Color on line) a)- elementary tetrahedra fFCD liable to form a portion of a double helix due to the favourable concavities; b)- abuting of several tetrahedra.

Fig. 11. Edge dislocations mobile in the plane of a perfect ellipse (belonging to a ideal FCD) and attached to it. The consecutive modification of the FCD results from a relaxation process towards a new ideal FCD; this process has to respect the boundary conditions, e.g. e = const. if the misorientation ω is fixed.

Fig. 12. The classic Volterra process for a rotation vector $\mathbf{\Omega}$ attached to O. At a point P on the cut surface, the lips of the cut surface suffer a relative displacement $\boldsymbol{d}_P(O) = \Omega \times \mathbf{OP}$.

Fig. 13. The extended Volterra process for a rotation vector $\mathbf{\Omega}$ attached locally to each point on £. Infinitesimal dislocations are attached all along the disclination line.

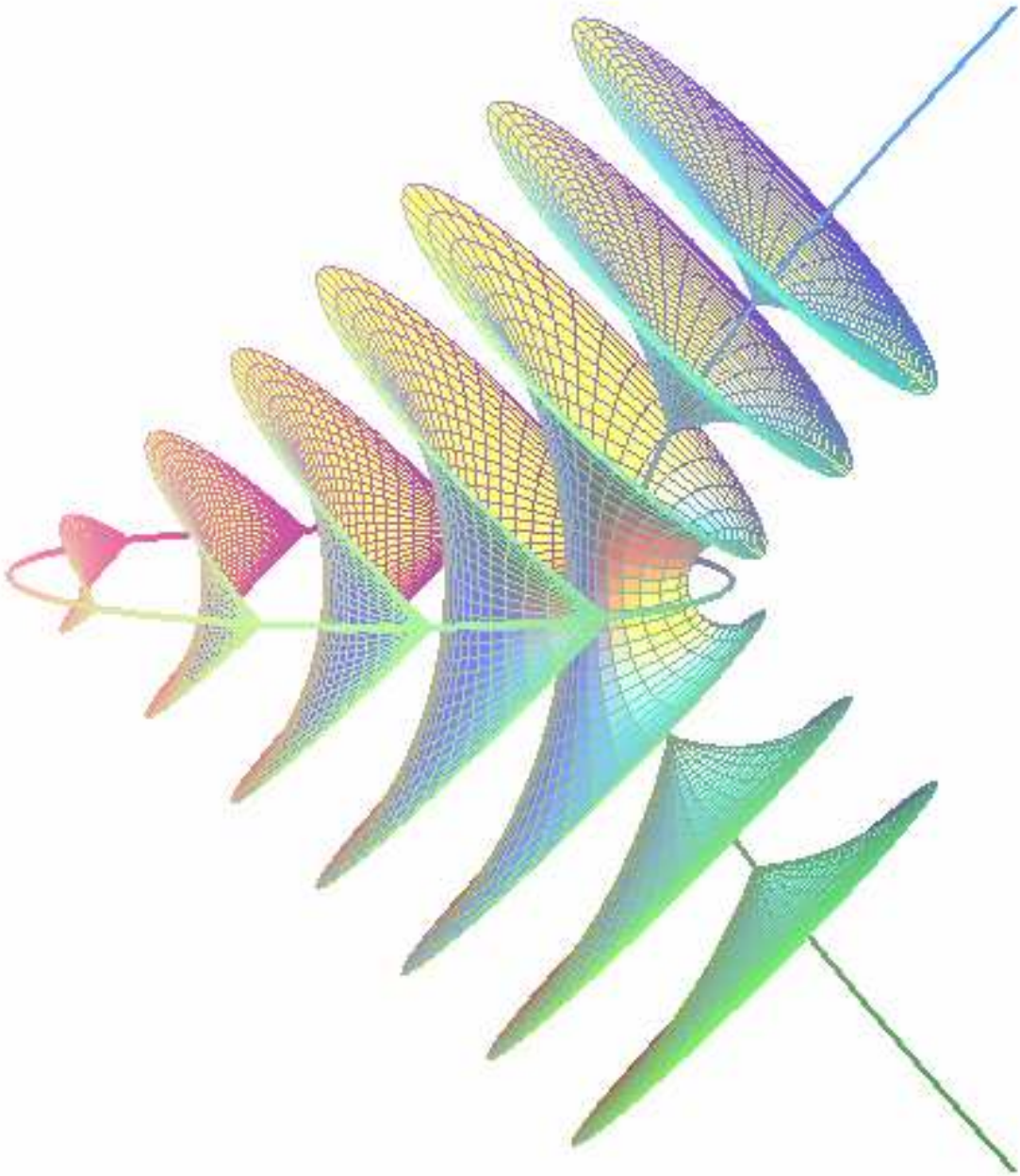

Fig. 1a, Kleman *et al.*

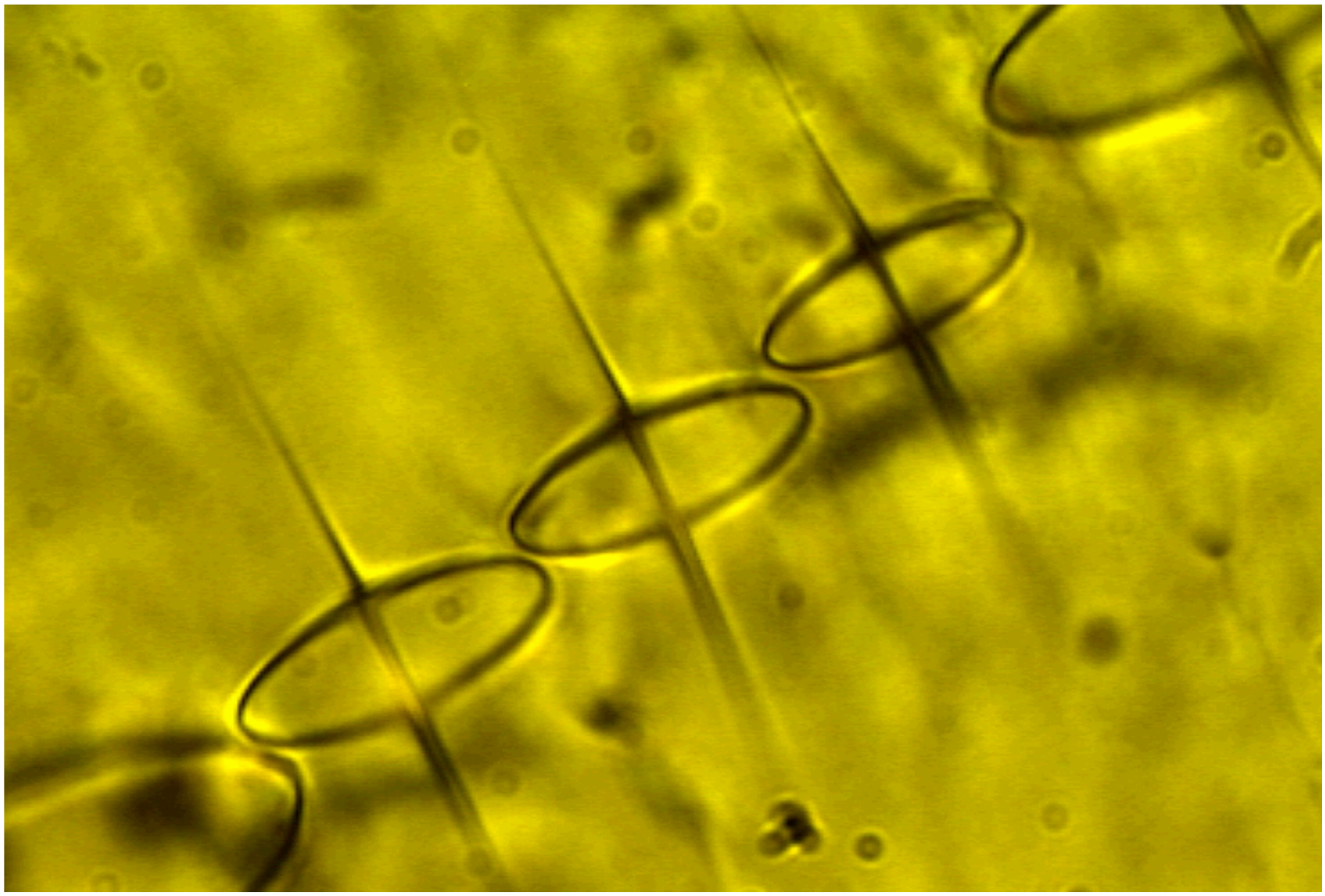

Fig. 2a, Kleman *et al.*

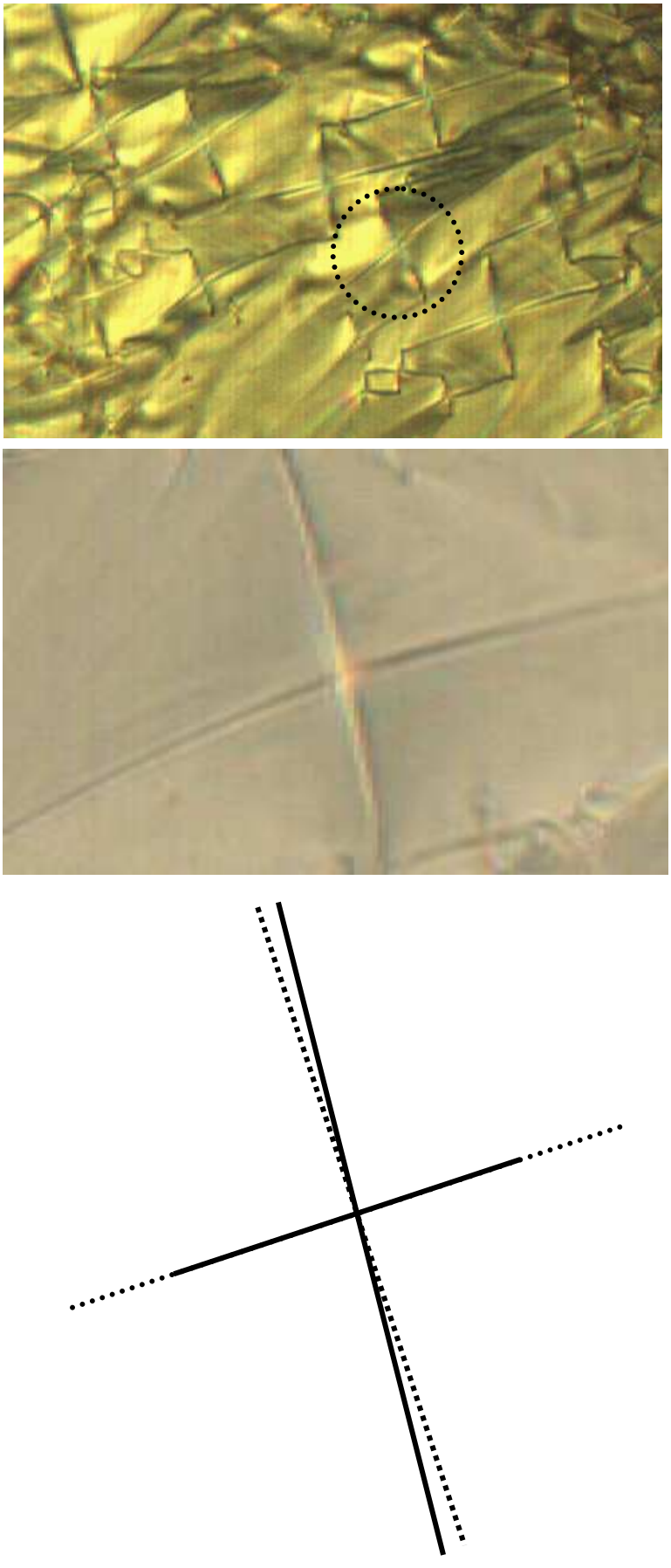

Fig. 2b, Kleman *et al.*

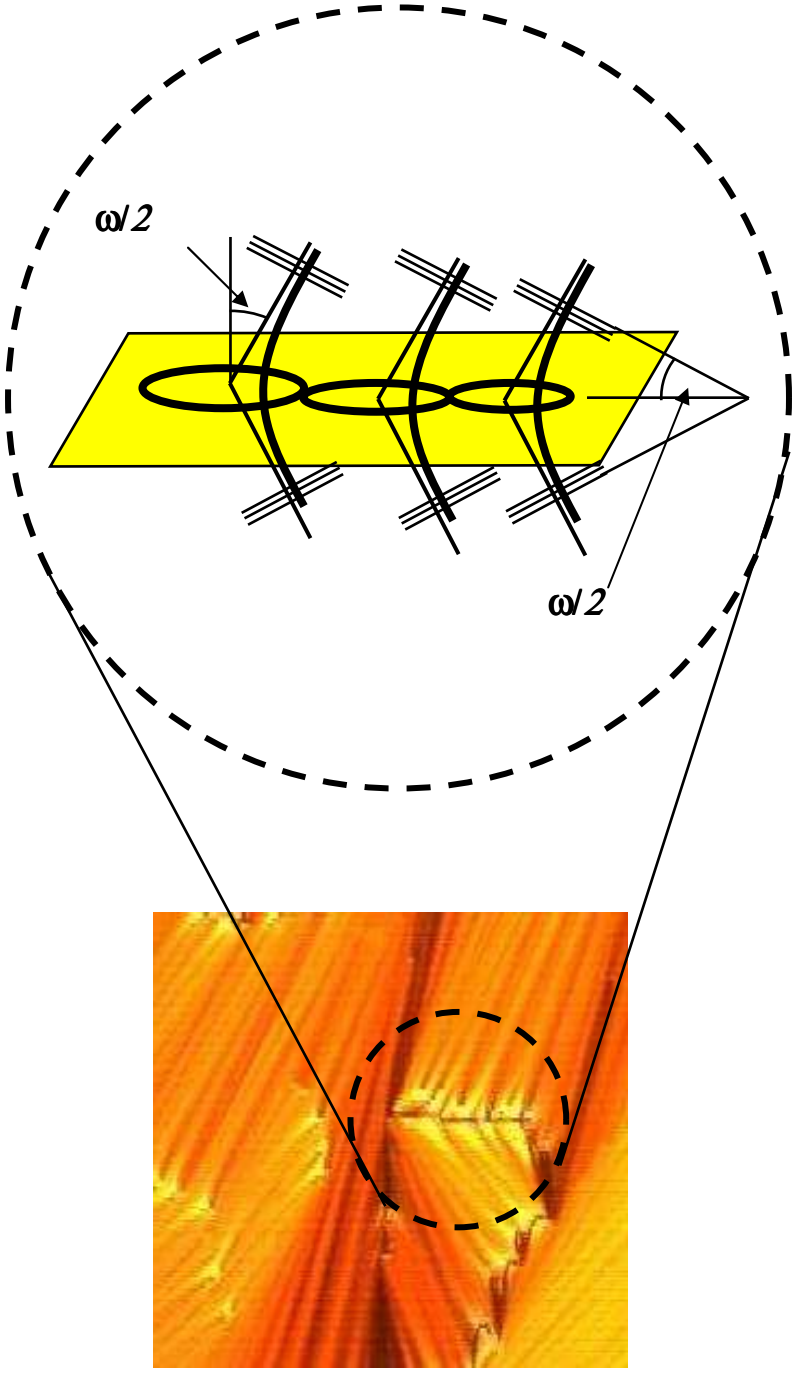

Fig. 3, Kleman *et al.*

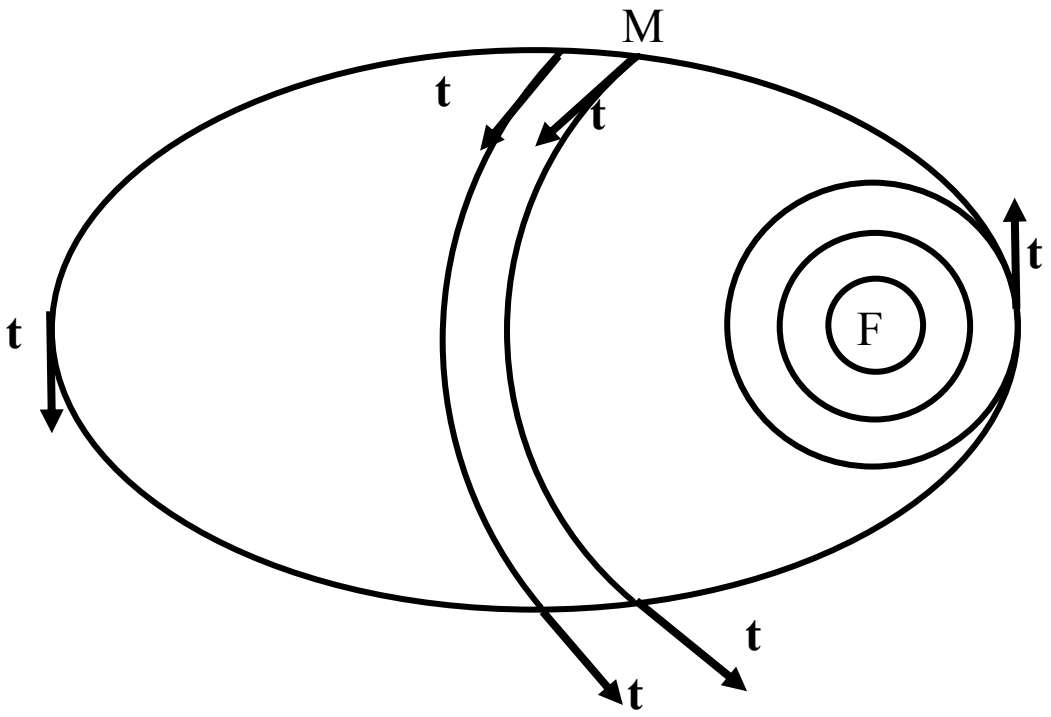

Fig. 4, Kleman *et al.*

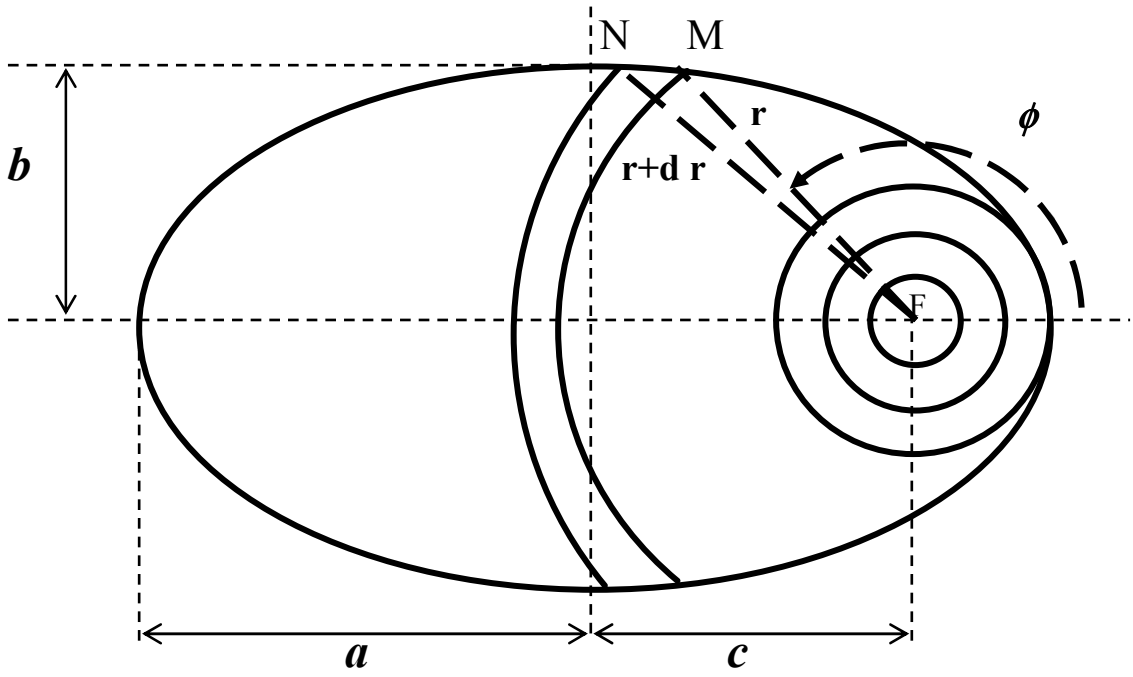

Fig. 6, Kleman *et al.*

8CB, thick free standing films

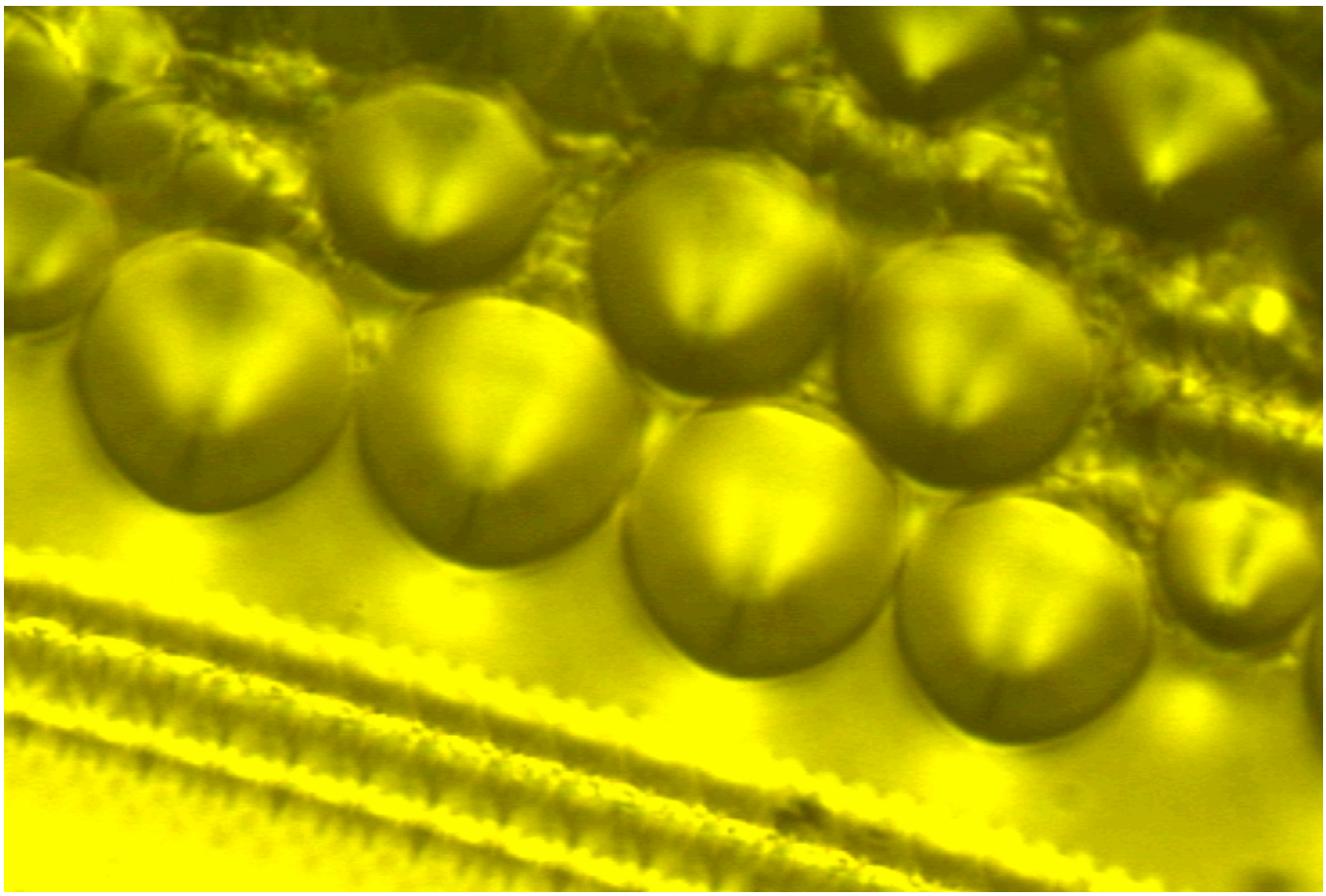

Fig. 7a, Kleman et al.

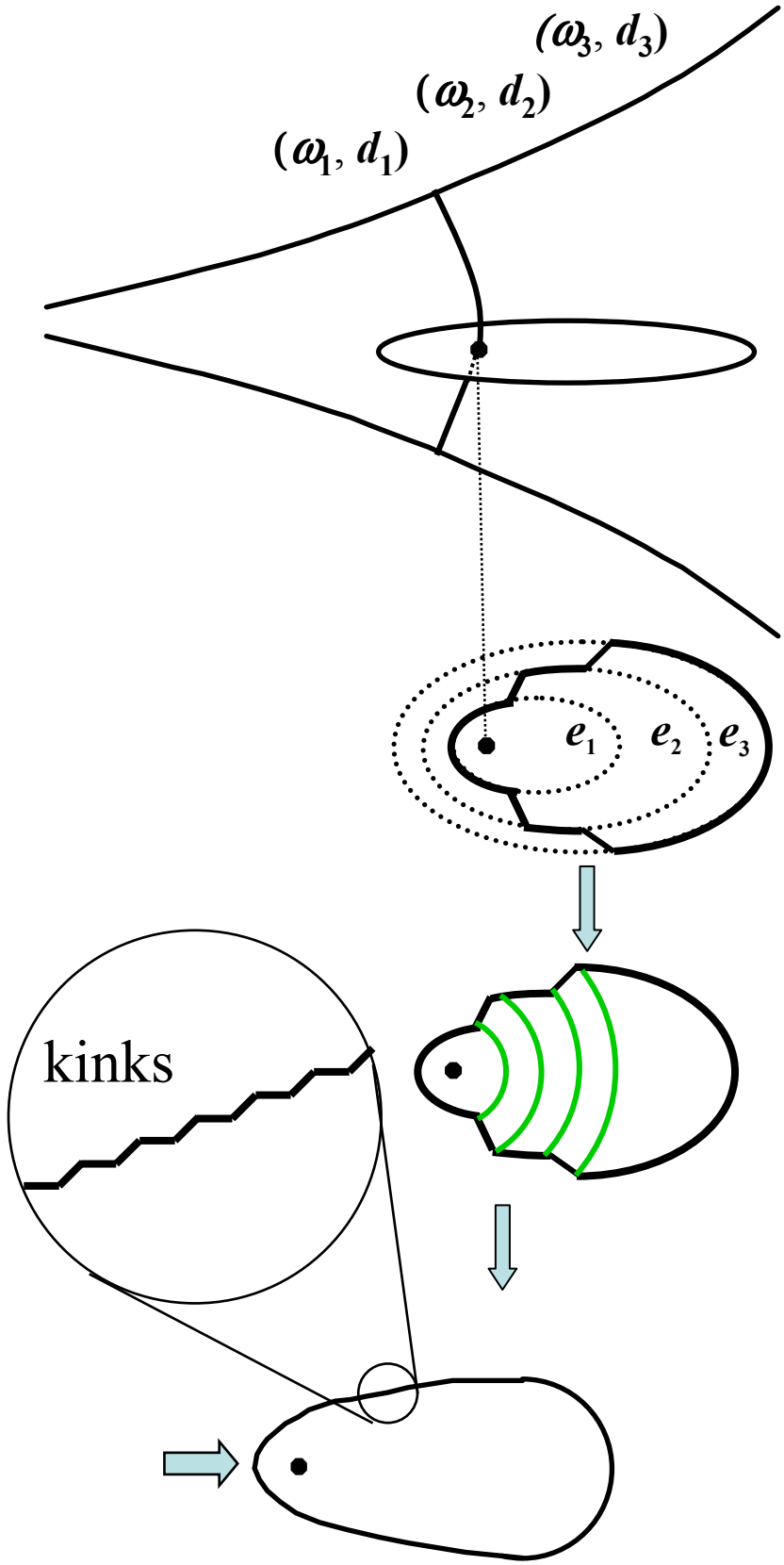

Fig. 7b, Kleman *et al.*

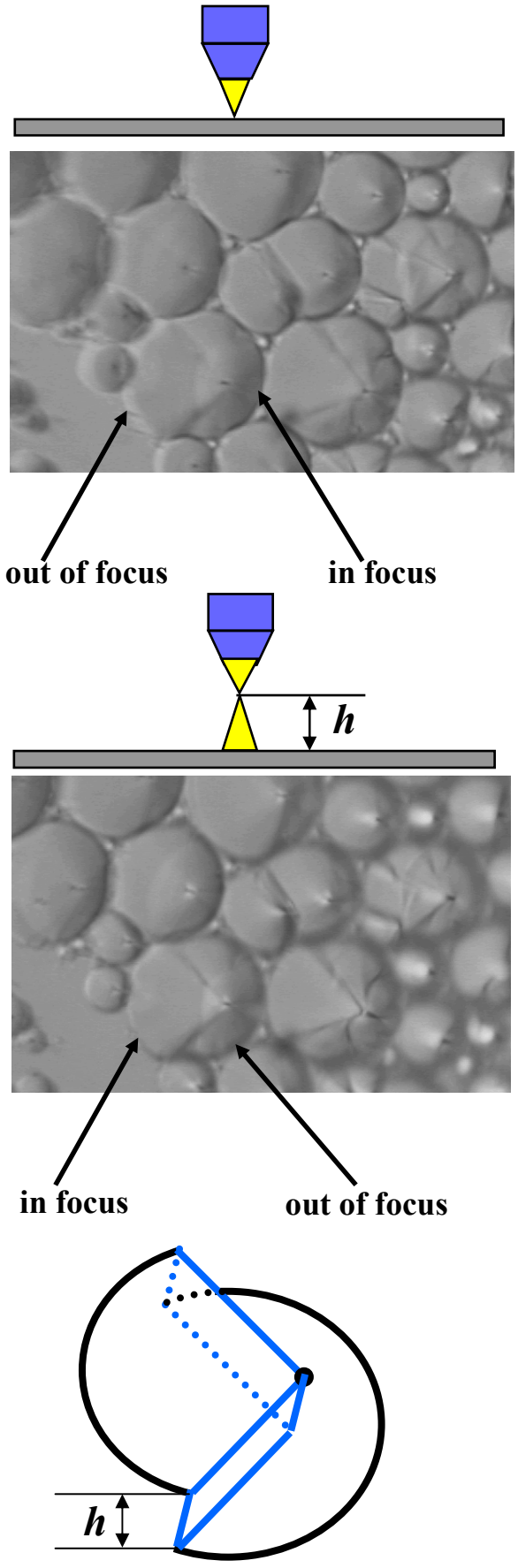

Fig. 8a, Kleman *et al.*

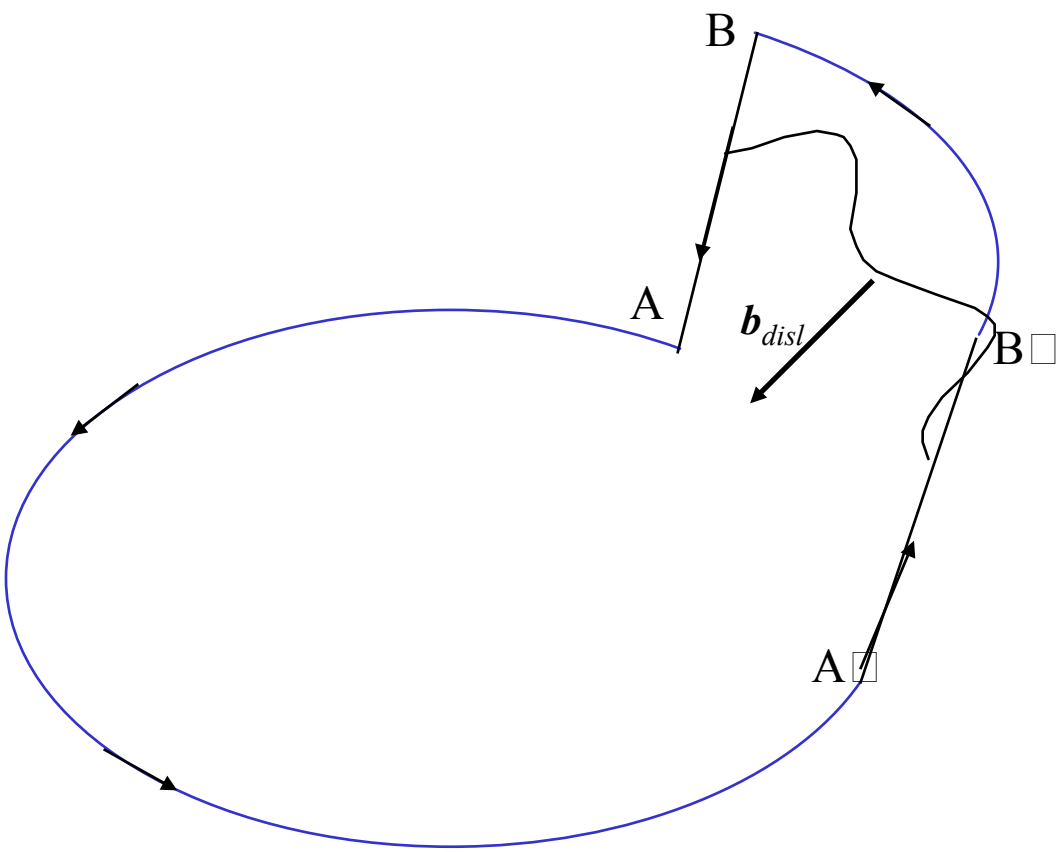

Fig. 8b, Kleman *et al.*

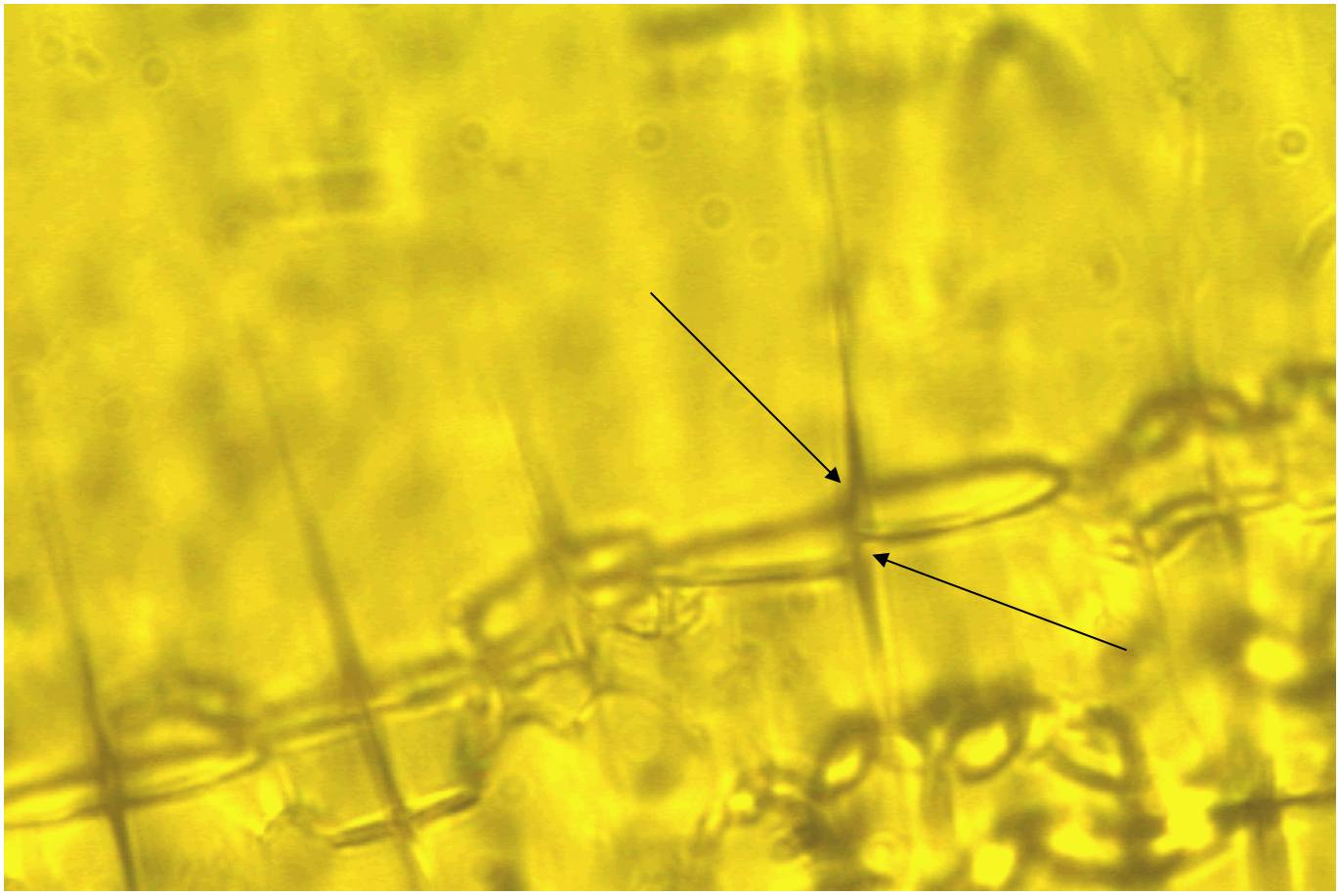

Fig. 8c, Kleman *et al.*

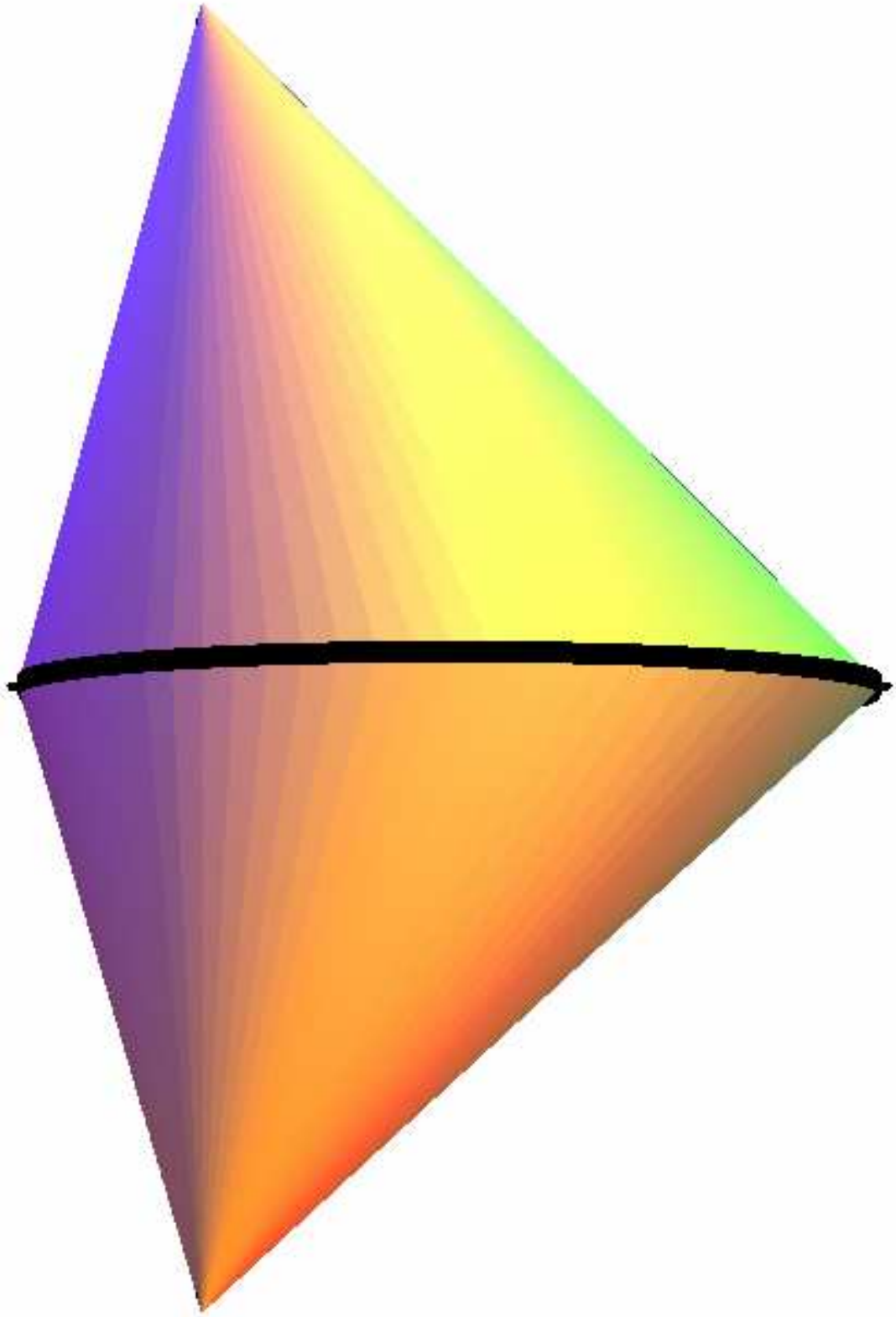

Fig. 9a, Kleman *et al.*

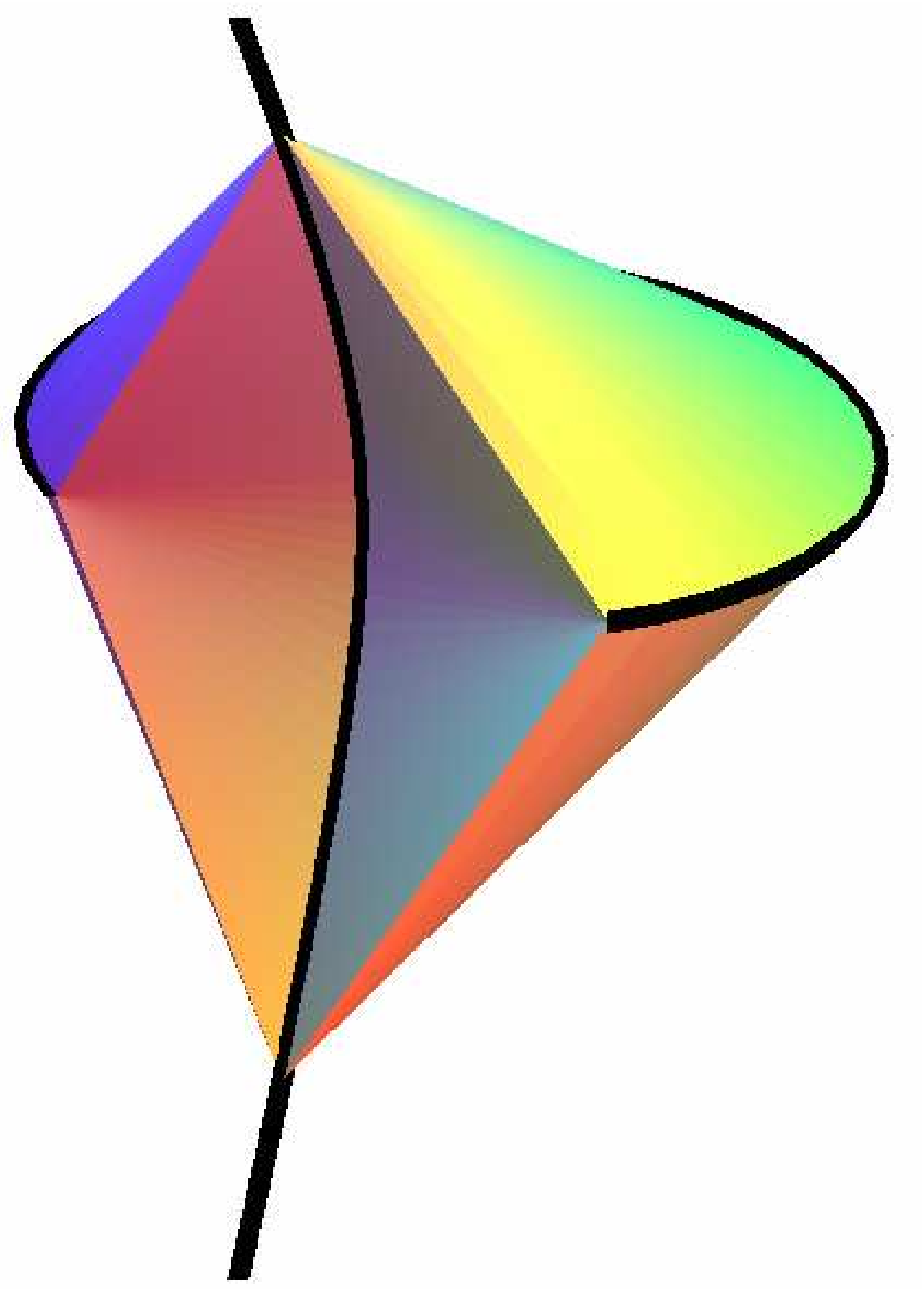

Fig. 9b, Kleman *et al.*

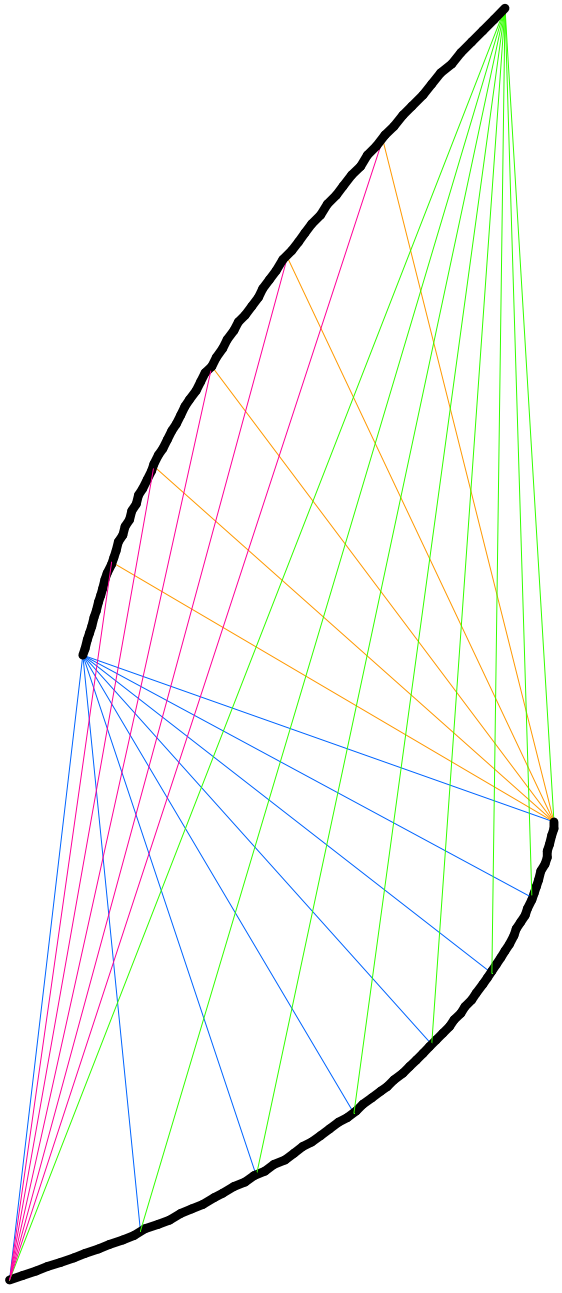

Figure 10a, Kleman et al.

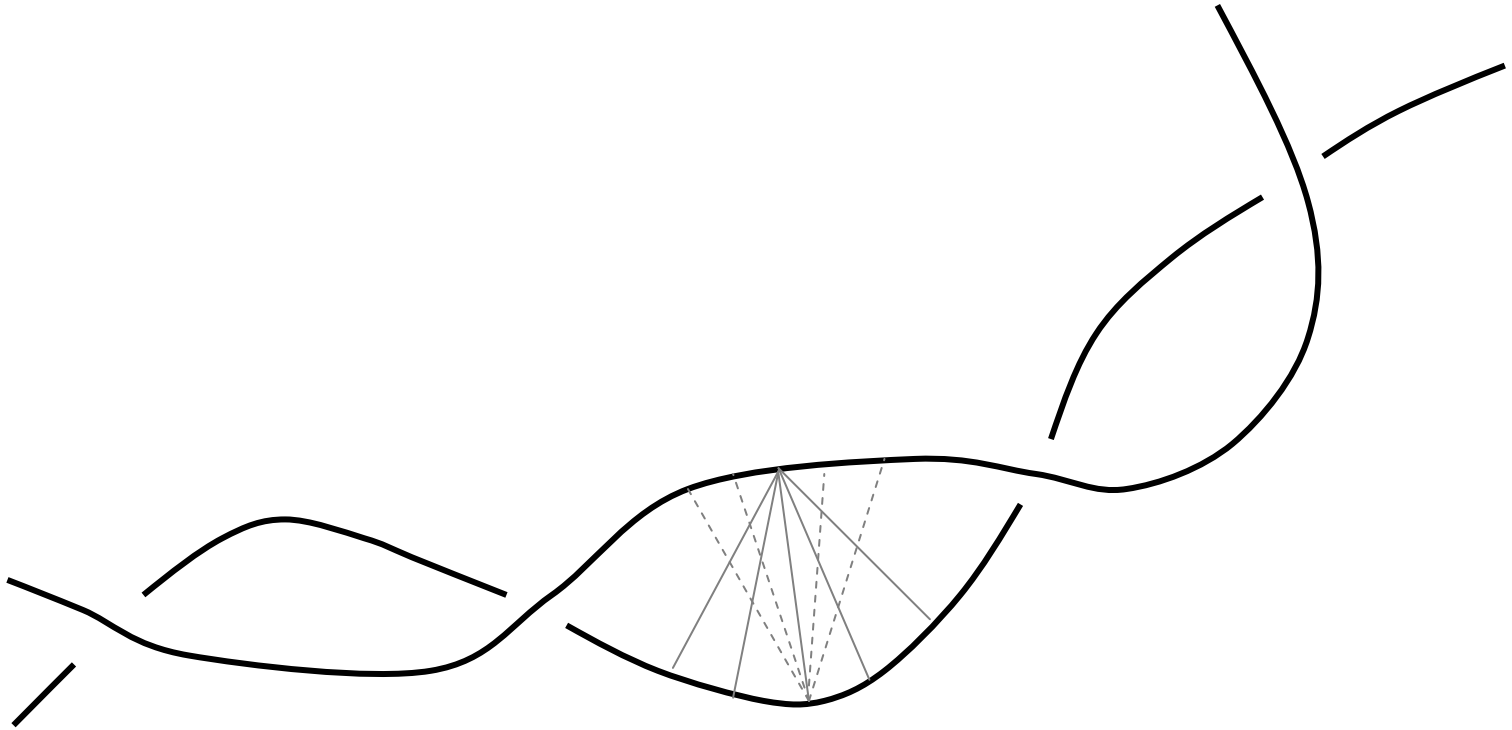

Figure 10b, Kleman et al.

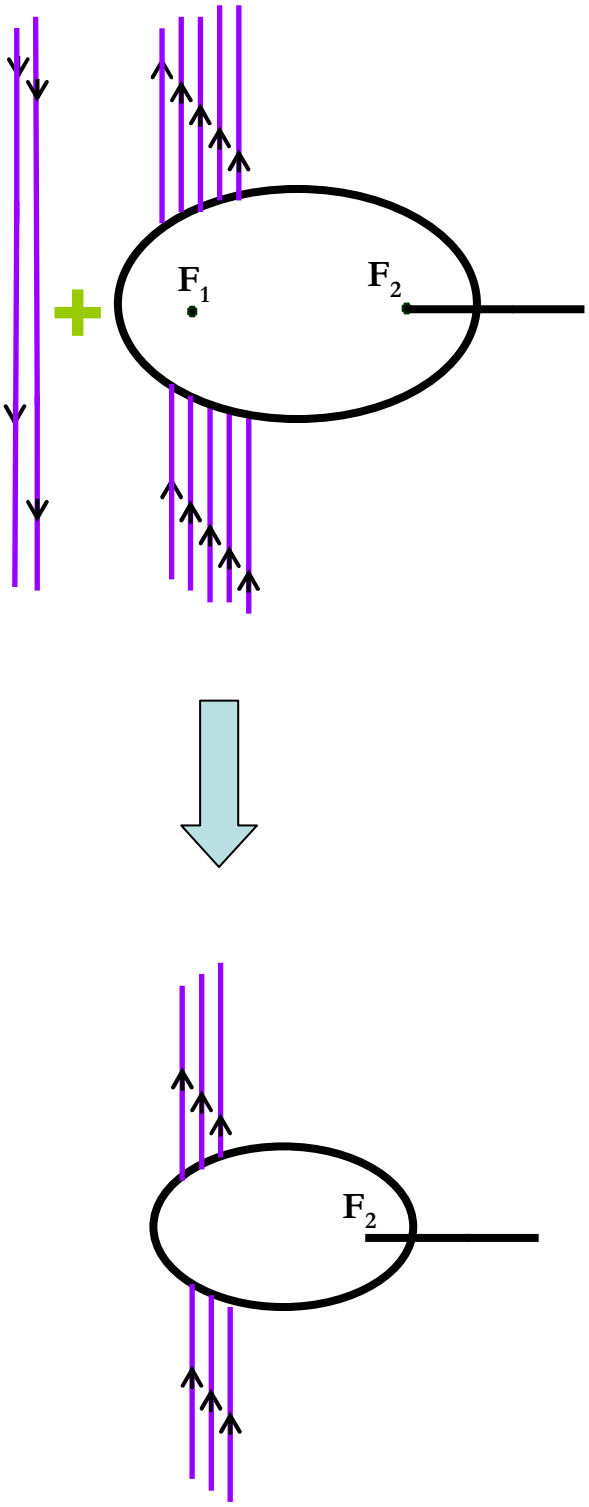
F1
F2
F2

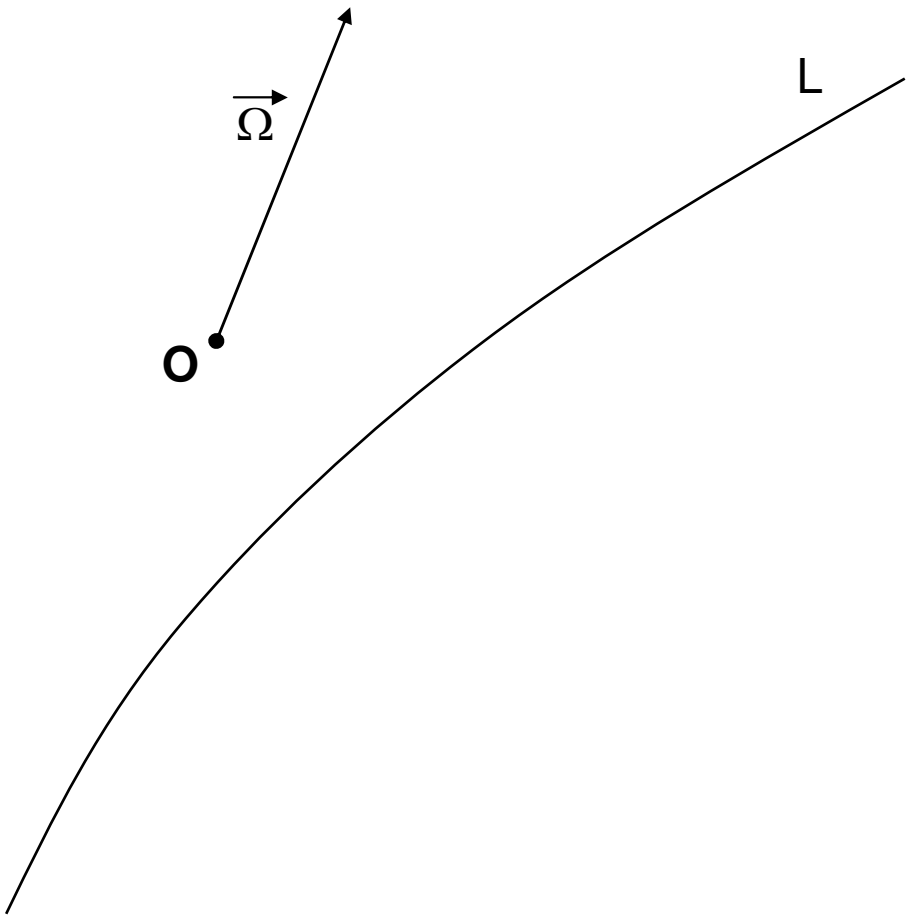
L
$\overrightarrow{\Omega}$
O

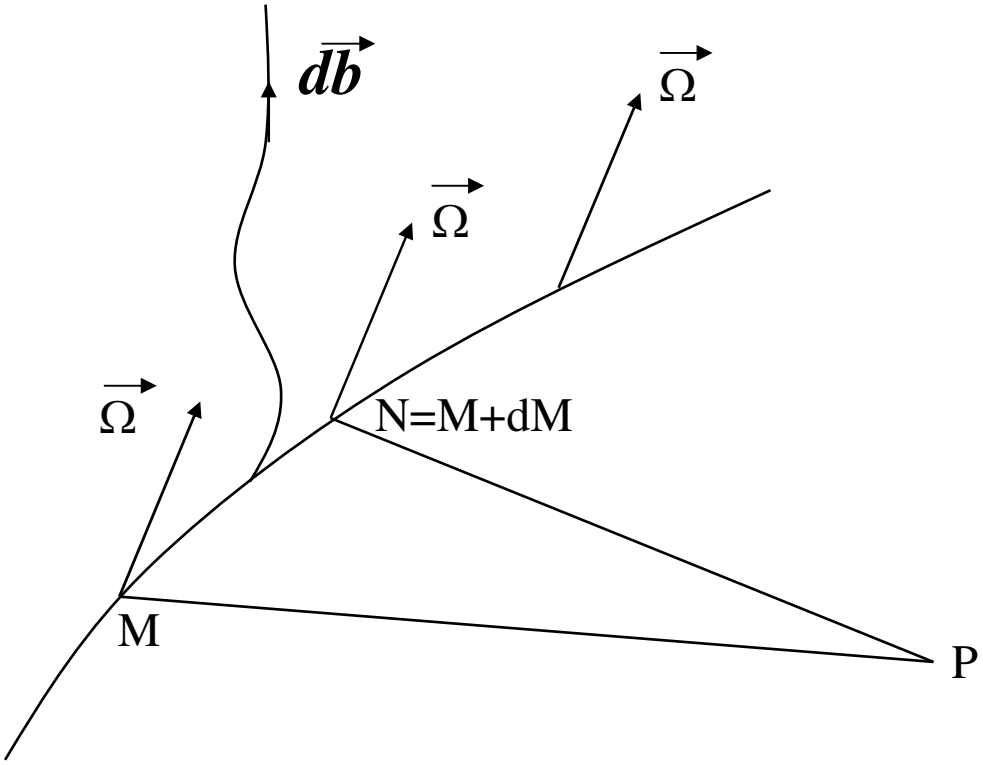
$\vec{db}$
$\vec{\Omega}$
$\vec{\Omega}$
$\vec{\Omega}$
N=M+dM
M
P